

Inertial Sensor Assisted Acquisition, Tracking, and Pointing for High Data Rate Free Space Optical Communications

Shinhak Lee and Gerry G. Ortiz
 Jet Propulsion Laboratory/California Institute of Technology
 Pasadena, CA 91109

ABSTRACT: We discuss use of inertial sensors to facilitate deep space optical communications. Implementation of this concept requires accurate and wide bandwidth inertial sensors. In this presentation, the principal concept and algorithm using linear accelerometers will be given along with the simulation and experimental results.

INTRODUCTION

High data rate, narrow beam free-space optical communications imposes the challenging task of precisely pointing the downlink beam to a fraction of the beam divergence. The required accuracy is typically less than a microradian in jitter and bias. This, in turn, requires a reference optical source, or a beacon in order to close the tracking/pointing control loop. To properly maintain the link, several kHz of beacon tracking rate has been required in the past Acquisition, Tracking, and Pointing (ATP) system design. The required tracking rate depends on the signal strength of the reference source and the platform vibration amplitude and frequency content. However, a fast beacon-tracking rate is not readily available in most deep space applications due to the limited beacon energy collected at the spacecraft (S/C) telescope.

The key to this problem is to compensate for the relative beacon movements measured on the Focal Plane Array (FPA). This is mostly due to spacecraft vibrations, rather than to the absolute beacon movements. Spacecraft vibrations make the beacon

appear to move around on the FPA. Therefore, accurate measurement of the spacecraft vibrations would allow relative beacon movements between reference beacon centroids to be deduced. If the error between the true and the estimated beacon positions is smaller than the error budget, the fast tracking rate can be maintained. Implementation of this concept requires accurate and wide bandwidth inertial sensors. Inertial sensors are available in many forms including linear and angular accelerometers, angular rate sensors, angle displacement sensors, and gyros.

In this work, three linear accelerometers were used to estimate x and y beacon positions. The approach of using accelerometers provides an alternative to other inertial sensors such as gyros, with the advantages of low cost, small size, and less power consumption. One of the drawbacks of this approach is the added complexity in the tracking algorithm, mainly in the estimation of angular (beacon) positions from the acceleration (i.e., platform vibration) measurements. Double integration of the acceleration using the trapezoidal method (Figure 1) and the triangular configuration of the three accelerometers (Figure 2) were used to estimate the angular positions.

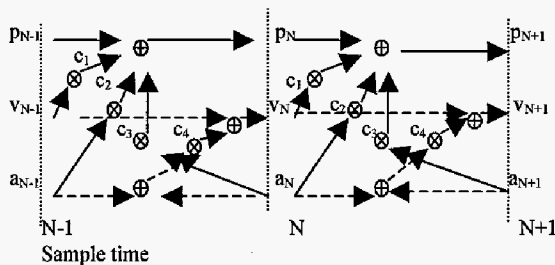


Figure 1. The linear position estimation procedure of APEA using acceleration measurements of a_i 's. p_i 's and v_i 's are i^{th} position and velocity, respectively. Multipliers (c_1 to c_4) are: $c_1 = \Delta t$, $c_2 = \Delta t^2/3$, $c_3 = \Delta t^2/6$, $c_4 = \Delta t/2$.

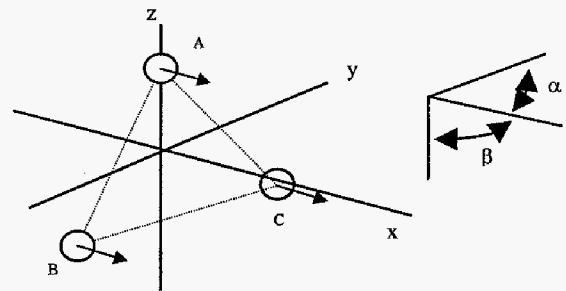


Figure 2. Triangular configuration of three accelerometers of A, B, and C to estimate two angular positions of α and β

ANGULAR POSITION ESTIMATION ALGORITHM

Due to the double integration, the initial velocity needs to be estimated. Also, the acceleration bias, due to any potential misalignment of accelerometers, needs to be corrected. The least square fit was used to estimate the initial velocity and acceleration bias. The block diagram depicting the APEA (Angular Position Estimation Algorithm) is shown in Figure 3. The performance of the angular position estimation algorithm (APEA) depends on the various error sources, which include sensor electronic noise, amplifier noise, quantization (sampling) noise, and algorithm error.

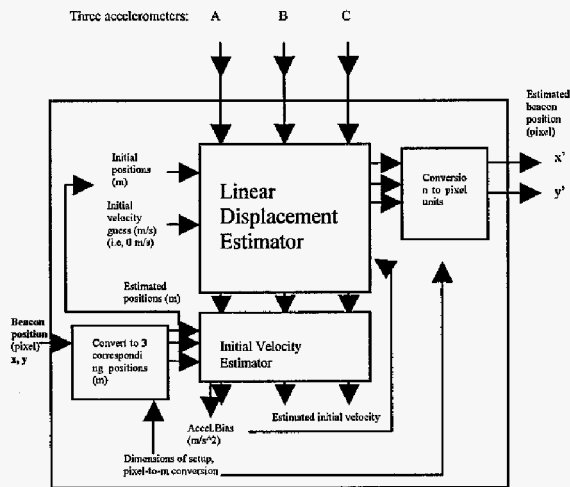


Figure 3. Block diagram of the APEA showing signal flows.

SIMULATION AND EXPERIMENTAL RESULTS

In a laboratory demonstration, other noise sources such as ambient room vibration, acoustic noise, and electromagnetic radiation impose an additional challenge. Error analysis showed that the estimation error is proportional to the measurement noise. The estimation error also increases with the frequency and amplitude of the vibration. Figure 4 shows the setup for the experiments. The injected vibration signal for the simulation and experiments is 30 Hz sine wave with amplitude of +/- 4.5 pixels (each pixel = 3.61 urad). For simulation (Figure 5), acceleration measurement noise of 1.2 mg was added to simulate the noisy laboratory environment. Figure 6 is the experimental result with the 30 Hz sine wave and

amplitude of +/-4.5 pixels. The RMS estimation errors are: 1.21 pixels from the simulation and 1.16 pixels from the experiments, respectively.

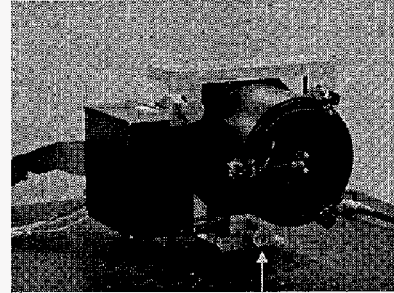


Figure 4. Three accelerometers (indicated by arrows) were mounted JPL optical communications demonstrator for the experiments.

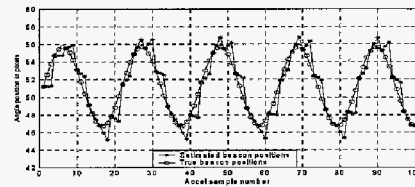


Figure 5. Simulation results for 30Hz vibration signal with noise equivalent to accelerations of 1.2 mg.

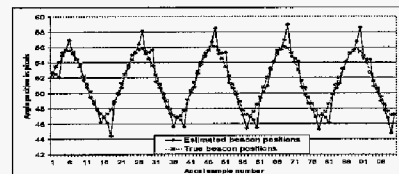


Figure 6. Experimental results for 30Hz vibration signal

ACKNOWLEDGEMENT

The research in this report was carried out by the Jet Propulsion Laboratory, California Institute of Technology, under contract with the National Aeronautics and Space Administration.